Full Title: Tailoring optical metamaterials to tune the atom-surface Casimir-Polder interaction

Authors
Eng Aik Chan,[1,2] Syed Abdullah Aljunid,[1] Giorgio Adamo[1], Athanasios Laliotis[3], Martial Ducloy*[1,2,3], David Wilkowski*[1,2,4,5]

Affiliations
[1] Centre for Disruptive Photonic Technologies, TPI, Nanyang Technological University, 637371 Singapore.
[2] School of Physical and Mathematical Sciences, Nanyang Technological University, 637371, Singapore.
[3] Laboratoire de Physique des Lasers, UMR 7538 du CNRS, Université Paris13-Sorbonne-Paris-Cité F-93430 Villetaneuse, France.
[4] Centre for Quantum Technologies, National University of Singapore, 117543 Singapore.
[5] MajuLab, CNRS-UNS-NUS-NTU, Université Côte d'Azur, International Joint Research Unit UMI 3654, Singapore.
*Please address all correspondence to David Wilkowski: david.wilkowski@ntu.edu.sg or Martial Ducloy: martial.ducloy@univ-paris13.fr

Abstract

Metamaterials are fascinating tools that can structure not only surface plasmons and electromagnetic waves, but also the electromagnetic vacuum fluctuations. The possibility of shaping the quantum vacuum is a powerful concept that ultimately allows engineering the interaction between macroscopic surfaces and quantum emitters such as atoms, molecules or quantum dots. The long-range atom/surface interaction, known as Casimir-Polder interaction, is of fundamental importance in quantum electrodynamics but also attracts a significant interest for platforms that interface atoms with nanophotonic devices. Here we perform a spectroscopic selective reflection measurement of the Casimir-Polder interaction between a Cs($6P_{3/2}$) atom and a nanostructured metallic planar metamaterial. We show that by engineering the near-field plasmonic resonances of the metamaterial, we can successfully tune the Casimir-Polder interaction, demonstrating both a strong enhancement and reduction with respect to its non-resonant value. We also show an enhancement of the atomic spontaneous emission rate due to its coupling with the evanescent modes of the nanostructure. Probing excited state atoms next to non-trivial tailored surfaces is a rigorous test of quantum electrodynamics. Most importantly, engineering Casimir-Polder interactions represents a significant step towards atom trapping in the extreme near-field, possibly without the use of external fields.

Introduction

Material boundaries modify the surrounding quantum vacuum giving rise to interactions between classical macroscopic surfaces (Casimir effect), or between a surface and a quantum polarizable object (Casimir-Polder interaction) [1]. The surface, inducing a shift of atomic energy levels, was investigated experimentally with thermal vapors [2], [3], [4], atomic beams [5], [6] and cold atoms [7],[8] [9]. The dispersive energy shift goes hand in hand with a dissipative change of the atomic radiative properties, allowing for the tuning of spontaneous emission rates of atoms next to dielectric surfaces. For this purpose placing atoms next to tailored nanostructures is becoming a new challenge in the field of nanophotonics. Hybridization of atomic and nanophotonic systems paves the way to novel quantum devices due to strong atom-light coupling with micro-cavities [10] or due to collective effects arising from strong confinement [11], [12]. The most common hybrid platforms include tapered nanofibers [13], hollow core fibers [14], or photonic bandgap waveguides [15].

The Casimir-Polder force has been largely perceived as an obstacle for placing atoms close to surfaces. Nevertheless, ambitious proposals emerge that suggest the possibility of utilizing atom-surface interactions to achieve tight trapping at record distances from surfaces [16] and in particular photonic bandgap waveguides [17], [18]. The tantalizing possibility of subwavelength atom trapping is made more difficult due to the predominantly attractive nature of the Casimir-Polder interaction that does not allow stable trapping potentials in all directions. Experimental demonstration of an efficient tuning of the atom-surface interaction, particularly between attraction and repulsion represents therefore a milestone in the field of hybrid systems.

Among the various approaches to modify the Casimir-Polder interaction, one relies on the resonant coupling between excited atoms and surface resonances. Thus, experiments with Cesium atoms in high lying excited states next to a sapphire surface have demonstrated resonant Casimir-Polder repulsion [19], [20] or an exaltation of the Casimir-Polder attraction with temperature [21]. The key parameter here, that governs both strength and sign of the Casimir-Polder interaction, is the relative detuning of the surface resonance frequency compared to the predominant atomic dipole coupling (transition). Active engineering of the atom-surface interaction is therefore severely limited by the selection of dielectrics that are available in nature. The possibility of exploring material birefringence as a means of tuning the polariton resonances has been proposed [22], but the theoretical tunability is restricted and yet to be demonstrated experimentally.

An alternative solution would be to use nanostructured periodic planar metamaterials that allow a broad tunability of plasmonic surface resonances across the visible and near infrared spectrum. This spectral domain, where plasmonic or polaritonic resonances are usually scarce in bulk material, is of particular interest since it matches with low-lying transitions of alkali atoms, routinely used in laser cooling or atomic spectroscopy experiments. Moreover, thin metallic planar metamaterials have enhanced light transmission at the plasmon resonance. It thus becomes possible to perform reflection spectroscopy on a vapor/metamaterial interface. Previous experiments on Cesium vapor demonstrated a modification of the surface reflectivity, however, analysis of the Doppler broadened spectra did not provide quantitative information on the frequency shift or the atomic lifetime modification at the proximity of the metamaterials [23], [24].

In this work, we report on high resolution frequency modulated selective reflection spectroscopy of $Cs(6P_{3/2})$ atoms in vicinity of a wide range of metallic planar metamaterials. The theoretical treatment of selective reflection on flat dielectric surfaces [25] is here further developed, allowing

us to measure the dispersive Casimir-Polder shift of the $6S_{1/2}\leftrightarrow 6P_{3/2}$, Cesium D2 transition as well as a dissipative modification of the spontaneous emission rate [26]. For an adequately chosen metamaterial, the frequency shift on the Cesium transition, induced by the Casimir-Polder interaction, can be almost suppressed. A QED calculation of the fully retarded Casimir-Polder interaction is shown to reproduce the basic features of our experimental data.

Results

The system under investigation, similar to the one used in [24], is depicted in Fig.1a. A Cesium vapor at T=80ºC is introduced into a vacuum chamber. The density of the atoms is around $N=10^{17}$ m^{-3} whereas the thermal velocity is $\bar{u}=150ms^{-1}$. On one of the dielectric viewports of the vacuum chamber, ten different metamaterials are engraved on a 50nm thick silver layer (see Fig.1b). Each metamaterial consists of a 200µm x 200µm square area containing arrays of 70 nm wide nanoslits of varying length from 170 to 240 nm. The unit cells are squares with sizes from w = 380 to 520 nm long, depending on the length of the slit. We achieve plasmonic resonances, characterized by their central position, covering a wavelength range from 670nm to 980nm. Each plasmon resonance has a typical width of 60nm (see an example in Fig.1c). The atoms/metamaterial hybrid system is excited and probed on the $6S_{1/2}\leftrightarrow 6P_{3/2}$ cesium D2 transition at 852nm, using a Selective Reflection (SR) optical setup at normal incidence [2], [27], [28].

The radiation is produced by an external cavity diode laser (ECDL). Part of the light is sent to a saturated absorption spectroscopy setup used as a frequency reference. The main beam goes through an Electro-Optic Modulator (EOM) to modulate its phase at $\omega_m/2\pi$ =9MHz with a modulation index of β=0.19 and is then shaped by a square mask to optimize its overlap with the metamaterial. The intensity of the laser is maintained below saturation, typically $I=1mW/cm^2$. The reflected light beam is collected on a fast and sensitive amplified photodetector. The signal at 9MHz is demodulated using a lock-in amplifier, directly providing the in-phase and in-quadrature component of the reflection signal, which is purely Doppler-free and analyzed in the following.

First, we analyze the reflectance and transmittance of the metamaterials at 852 nm using the ECDL. To do so, we detuned the laser away from the cesium resonance such that it is not coupled anymore to the atomic vapor whereas the coupling to the plasmon remains unchanged. The results are summarized in Fig.2. Here, each pair of reflectance/transmittance data corresponds to a given metamaterial, which is characterized by its center resonance frequency, λ_p, reported on the x-axis of the graph. The resulting curves show a smooth resonance-like behavior, indicating that all the metamaterials have a similar reflectance and transmittance spectrum (see also [24]). For a more quantitative analysis, we perform a Finite Difference Frequency Domain (FDFD) simulation of the metamaterials. We extract the expected far-field reflectance and transmittance intensities of the metamaterials. The FDFD results are in good quantitative agreement with the experimental data. However, we perform a global adjustment of the contrast of the reflectance and transmittance of the FDFD results by a factor of 0.7 and 0.5 respectively. This adjustment accounts for frequency independent optical losses, not encountered in the FDFD simulation. Contributions may come from photon scattering at the metamaterials, imperfect size matching of the beam to the metamaterial or possible long-range inhomogeneity of the metamaterial geometry.

We now tune the laser onto the $F=4\leftrightarrow F'=5$ hyperfine transition scanning over a frequency range of 100MHz $=\sim 20\Gamma$, where Γ = 5.2MHz, is the bare frequency width of the atomic transition. The

demodulated signals at 9MHz of the beam reflectance correspond to the red points on Fig.3. We observe a strong modification of the Doppler-free spectrum due to the presence of the metamaterials with respect to a plain dielectric window (see blue points on Fig.3). The hyperfine structure of the D2 line is spectrally resolved with our selective reflection experiment, as the frequency spacing between hyperfine components (200MHz between F'=3 and F'=4 and 250MHz between F'=4 and F'=5) are much larger than the width of the observed spectra (~10-20MHz). Also, the plasmonic resonance is much broader than the hyperfine splitting therefore its effects are identical on all hyperfine components. Similar selective reflection spectra can be obtained for the F=4↔F'=3,4 transitions albeit with a smaller amplitude due to weaker transition probabilities.

To further analyze the experimental data, we model the metamaterial by a spatially homogeneous bulk material having the same thickness and far-field reflectance/transmittance at normal incidence. This mean-field approximation holds for the thermal vapor at the vicinity of the metamaterial because the large spatial variation of the plasmon (see example in Fig.1d) is well smoothed by the finite response time of the atomic coherence (see Supplementary Materials for more details).

In SR spectroscopy with a homogeneous material interface, the vapor can be characterized by an effective electric susceptibility, χ. Its frequency derivative is given, in the Doppler limit ($k\,\bar{u} \gg \Gamma$), by [25] :

$$\frac{d\chi(\omega)}{d\omega} = i\frac{2Nk\mu^2}{\sqrt{\pi}\,\bar{u}\,\epsilon_0\hbar}\int_0^\infty dz \int_0^\infty dz' \,\frac{(z-z')e^{ik(z+z')}}{\mathcal{L}_o(\omega,z)-\mathcal{L}_o(\omega,z')} \tag{1}$$

$\frac{\mathcal{L}(\omega,z)}{z} = \frac{\Gamma}{2} - i\left(\omega - \omega_o + \frac{\Delta C_3 z^{-3}}{2}\right)$ is the Lorentzian lineshape of the bare atomic resonance, corrected by the z^{-3} Casimir-Polder frequency shift in the non-retarded regime. Here, ω_o is the bare atomic resonance, k is the wavenumber of the laser beam and μ is the two-level atomic dipole moment. Spectroscopic experiments are sensitive to the energy difference between levels. We therefore denote ΔC_3 the difference of van der Waals coefficients between lower and upper state. In our analysis, ΔC_3 is considered to be complex. As can be seen from the equations above, its real and imaginary parts denote a distance dependent shift and linewidth respectively. The metamaterial/vapor interface is located at z=0. We note that the phase factor, $e^{ik(z+z')}$ rapidly averages the effective susceptibility to zero for $z, z' >> k^{-1}$. As an important consequence, only the atoms located in a layer of thickness k^{-1} contribute to the SR signal. Moreover, as it can be seen in Eqn.1 and already discussed above, the signal is Doppler-free. We note as well that, since $\chi << 1$, the index of refraction of the atomic vapor reads as $n=1+\chi/2$. Under this approximation, the complex reflection coefficient of the electric field for the dielectric/metamaterial/vapor system can be linearized as:

$$r = r_o + \rho\chi \tag{2}$$

where r_o and ρ depend only on the indices of refraction of the metamaterial n' and of the dielectric substrate n_d (see Materials and Methods). In the Doppler limit, $\chi(\omega)$ is obtained by integration of Eqn.1. In the weak modulation limit, i.e. $\beta << 1$ we find that the demodulated signal has the following expression for the in-phase signal [25]:

$$V_p(\omega) = V_0 Re\{r_0^*\rho[\chi(\omega+\omega_m) - \chi(\omega-\omega_m)]\} \tag{3}$$

and for the in-quadrature signal,

$$V_q(\omega) = V_0 Im\{r_0^* \rho[\chi(\omega + \omega_m) + \chi(\omega - \omega_m) - 2\chi(\omega)]\} \quad (4)$$

V_0 is a factor of proportionality. Within the mean-field approximation, the complex factor $r_0^* \rho$ can be evaluated analytically (see Materials and Methods for more details). It depends on n', n_d and the metamaterial thickness. By mixing the real and imaginary part of the susceptibility, the factor $r_0^* \rho$ gives the main contribution of the modification of the atomic resonance lineshape induced by the plasmon resonance observed in Fig.3. Also, the product of the susceptibility with complex value $r_0^* \rho$ in Eqn.3 and Eqn.4 leads to Fano-like resonance of the atoms/metamaterial hybrid system as shown by some of us in [24] and by Stern and co-authors using a Kretchman geometry [23]. In addition to the Fano-like resonance, the Casimir-Polder interaction induces an additional contribution on the SR signal that we are now aiming to reveal and discuss.

Using Eqns.1-4, we perform a fit of the SR signals for the different metamaterials including the bare dielectric substrate. The fitting parameters are the atomic resonance linewidth Γ, the complex value of ΔC_3 and a common V_0 value. The effective index of refraction of the metamaterial *n*', thus the factor $r_0^* \rho$ is extracted from the FDFD simulation [29], [30]. The results of the fitting procedure correspond to the black curves in Fig.3. We observed an excellent agreement with the experimental data. The volume atomic resonance width (away from the surface) is found to be $\Gamma/2\pi$=10(3)MHz, *i.e.* slightly larger than the bare linewidth of 5.2MHz. This increasing of the linewidth, encountered as well on the dielectric interface, has been also reported in similar studies [3]. It can be due to residual collisional broadening. Most importantly, an imaginary part for the ΔC_3 has to be considered. To illustrate this point, we perform another fit, setting $Im[\Delta C_3]=0$. Under this constraint, we observe that the convergence of the fitting procedure is not satisfactory (see residue comparison in Fig.3 for λ_p=858nm).

The complex van der Waals coefficients obtained from the fits are shown in Fig.4a-b. The real part of the ΔC_3 coefficient (Fig.4a), displays a dispersive type of resonant behavior centered at λ_p~840nm. At the blue side of the resonance we observe a significant increase of the interaction, with respect to its off resonant value ~ 5kHz μm^3, followed by a sharp decrease that leads to a nearly vanishing value of the interaction at the red side of the resonance. The resonance width is in agreement with the plasmon linewidth of 60nm, confirming the plasmonic origin of the modification of the ΔC_3 values. The presence and evolution of the imaginary (dissipative) part for the van der Waals coefficients, shown in Fig.4b, corresponds to a decreasing of the atomic lifetime associated with enhancement of the vacuum mode density at the plasmonic resonance. This enhanced emission rate can be also be understood as an increasing of the Purcell factor as observed for example with ultracold gas [31] or nano-antennas [32]. The enhanced radiation emission of the atom/metamaterial system can finally, either be coupled to electromagnetic propagating modes, or be lost due to Ohmic losses in the metal. The selective reflection technique does not distinguish between those two cases.

Discussion

We compare our experimental measurements, with the QED theory of atom-surface interactions. A complete analysis of the resonant Casimir-Polder interaction depends on the knowledge of the dielectric properties of the metamaterial for both real and imaginary frequencies. For this purpose, we fit the dielectric constant ε, extracted by FDFD simulations, to an analytical model that accounts for the resonances of the metamaterial as well as the surface plasmon resonance of silver itself. We then calculate the difference of the Casimir-Polder frequency shift between $Cs(6P_{3/2})$ and

$Cs(6S_{1/2})$, which is the experimentally measured quantity in SR spectroscopy. Here, we take into account both non-resonant and resonant components. The non-resonant term does not depend on the position of the plasmon resonance and is mostly governed by the metallic response over the entire frequency spectrum [33], [34]. The influence of the plasmon resonance is contained in the resonant contribution [34], [35], which is only relevant for the excited state $Cs(6P_{3/2})$ interaction potential. It concerns the resonant photons on the $6S_{1/2}\leftrightarrow 6P_{3/2}$ transition and it is mainly at the origin of the observed Casimir-Polder resonant behavior (see Supplementary Materials). The results of the non-retarded model are shown as dashed lines in Fig.4c-d. The theoretical predictions exhibit a resonant behavior similar to the experimental findings, showing that our model captures the essence of the physical mechanism behind the tuning of the atom-surface interaction. However, the amplitude of the resonance is smaller than the experimentally measured one.

In our experiments, the plasmonic resonances coincide with the probing selective reflection wavelength. This suggests that we are not in a pure near-field regime and that retardation effects cannot be neglected [36]. In the retarded regime the dephasing of the oscillating dipole with respect to its image causes the resonant term of the excited state to oscillate with a period of $\lambda/2$ (atomic transition wavelength) [33], [34]. The phase and amplitude of these oscillations depends on the surface reflection coefficient [36] which varies significantly with the plasmonic resonance of the metamaterial. For this reason retardation can affect the amplitude and the shape of the ΔC_3 resonance (see also Supplementary Materials). To strengthen our analysis further, we calculate an 'effective' van der Waals coefficient as a function of distance, defined as $C_3(z) = \frac{\delta E(z) z^3}{\hbar} + i\frac{\delta\Gamma(z) z^3}{2\hbar}$, where $\delta E(z)$ is the Casimir-Polder shift and $\delta\Gamma(z)/2$ the linewidth of a given atomic level. We find that they both deviate significantly from the near field (van der Waals approximation) even at nanometric distances away from the metamaterial surface. Analysis of the SR lineshapes reveals that the relevant distance range is 70-100nm, in agreement with a characteristic probing depth $\sim \lambda/2\pi$. In Fig.4c-d we compare our experimental results with the real and imaginary parts of an effective $\Delta C_3(z)$ coefficient for distances between 70nm and 100nm, where $\Delta C_3(z)$ is the difference between the 'effective' van der Waals coefficients of excited ($6P_{3/2}$) and ground states ($6S_{1/2}$). Retardation effects enhance the amplitude of the ΔC_3 resonance but fail to exactly reproduce the experimental data. It should be noted that our calculations were performed for a semi-infinite effective bulk material. However, considering a finite layer of 50nm has a minor impact on the ΔC_3 values (see Supplementary Materials for more details). We also mention that the real and imaginary parts of the ΔC_3 coefficient in the case of pure silver are ~4.5kHzμm^3 and ~0.5kHz μm^3 respectively. This is in agreement with the experimentally measured off-resonant values of the coefficient, confirming the validity of our data analysis. We finally note that in our mean field analysis we have considered a homogeneous metamaterial, characterized by one effective dielectric constant. A future more detailed analysis would have to take the anisotropy of the metamaterial into consideration. For this purpose, the theoretical framework for anisotropic interactions described in [22] has to be expanded to include the effects of retardation.

To conclude, we use planar metamaterials as a testbed to control the Casimir-Polder frequency shift of the D2 line of Cs atoms. When the plasmon resonance almost coincides with the atomic resonance, the Casimir-Polder frequency shift nearly vanishes. Across the different metamaterials, the Casimir-Polder interaction is characterized by the usual real coefficient leading to a dispersive resonance, as well as a non-zero on-resonance dissipative response.

Finally, we mention that gratings have been previously used in Casimir [37], [38] as well as non-resonant Casimir-Polder experiments with Bose condensed ground state Rb atoms [39]. In these

cases, the experiments have strenuously tested various theoretical models/approximations for calculating vacuum forces with non-trivial surface geometries, demonstrating the non-additivity of the Casimir-Polder interaction at short distances. Our measurements are different since we explore resonant Casimir-Polder interactions with excited state atoms next to a silver metamaterial. It might be interesting to note that our results show that nano-patterning the silver surface, typically removing 7% of material, can in some cases increase the Casimir-Polder interaction by more than 100% with respect to pure silver. This is a powerful illustration of Casimir-Polder non-additivity. Our theoretical analysis, based on the mean field approximation, reproduces the main characteristics of the Casimir-Polder resonance albeit with a smaller amplitude. It would be worth comparing our experimental results with numerical models that fully account for the shape of the metamaterial.

Materials and Methods

sample fabrication

Our experiments are conducted in a vacuum chamber with metamaterial samples fabricated on one of the optical access windows of the chamber [24]. A quartz wedge window 3° is used to support a 50nm layer of silver deposited by thermal evaporation and protected by an 8nm layer of SiO_2. The metamaterials were then fabricated by focused ion beam milling. Each metamaterial array is 200µm x 200µm in size. We also fabricate a window in the silver film for reference measurements. The chamber base pressure is 10^{-8}mbar, whereas the cesium vapor pressure is maintained at a temperature of 80°C corresponding to vapor pressure of P = 10^{-4}mbar.

derivation of the $r_0^*\rho$ parameter

The reflection coefficient in the mean-field approximation is given by [40] :

$$r = \frac{(n_d-n')(n'+n)+(n_d+n')(n'-n)e^{\frac{2in'l\omega}{c}}}{(n_d-n')(n'+n)-(n_d+n')(n'-n)e^{\frac{2in'l\omega}{c}}} \tag{5}$$

where n_d, n' and n are respectively the index of refraction of the dielectric substrate, of the effective bulk material, (describing the metamaterial) and of the atomic vapor. l is the effective bulk material thickness. The index of refraction of the atomic vapor is given by $n = 1 + \chi/2$ where the atomic susceptibility χ. Since $\rho = \frac{\partial r}{\partial \chi}|_{\chi=0}$, the complex coefficient $r_0^*\rho$ is found to be:

$$r_0^*\rho = \frac{4|r_o|^2 n_d n'^2 e^{\frac{2in'l\omega}{c}}}{(1+n')^2\left(n'^2-n_d^2\right)+2(1-n'^2)\left(n_d^2+n'^2\right)e^{\frac{2in'l\omega}{c}}+(1+n')^2\left(n'^2-n_d^2\right)e^{\frac{4in'l\omega}{c}}} \tag{6}$$

calculation of the Casimir-Polder interaction

Here we calculate the Casimir-Polder interaction between an excited state atom and a metameterial using the perturbation approach first described in [33], [34], also followed in numerous other works. In the framework of the mean field approximation, metamaterials are considered uniform and isotropic materials with an effective dielectric constant extracted by FDFD simulations for a wavelength range between 500nm to 1500nm. Casimir-Polder calculations rely on the knowledge of the dielectric function at the entire frequency range and for this purpose, we fit the FDFD data using the following analytic function:

$$\epsilon(\omega) = 1 - \frac{\omega_p^2}{\omega^2+i\,\gamma_p\omega} + \sum_j \frac{f_j\omega_j^2}{\left(\omega_j^2-\omega^2\right)-i\gamma_j\omega} \tag{7}$$

The first part of the equation is a Drude model that accounts for the bulk properties of silver. The plasmon frequency ω_p and dissipation γ_p are common for all metamaterials. The second part models the metamaterial resonances. The amplitude (f_j), frequency (ω_j) and dissipation (γ_j) of each resonance is a smoothly varying function of the plasmonic resonance (λ_p) of the metamaterial. By interpolating these parameters we can calculate the Casimir-Polder interaction for a continuous range of metamaterials (see Fig.4c,d). We stress here that our calculation does not critically depend on the analytic model used to fit the dielectric constant. This is because the physics is mostly contained on the resonant part of the interaction which depends on $Re[\frac{\epsilon(\omega_o)-1}{\epsilon(\omega_o)+1}]$, where ω_o is the atomic resonance frequency. At zero temperature (T=0) the ground state potential as a function of distance z, writes:

$$\delta E(z) = -\frac{1}{\pi}\sum_n \omega_{gn}\mu_\alpha^{gn}\mu_\beta^{ng}\int_0^\infty d\xi \frac{G_{\alpha\beta}(z,i\xi)}{\xi^2+\omega_{gn}^2} \quad (8)$$

The excited state potential:

$$\delta E(z) = -\frac{1}{\pi}\sum_n \omega_{en}\mu_\alpha^{en}\mu_\beta^{ne}\int_0^\infty d\xi \frac{G_{\alpha\beta}(z,i\xi)}{\xi^2+\omega_{en}^2} - \sum_n \mu_\alpha^{gn}\mu_\beta^{ng} Re\big[G_{\alpha\beta}(z;|\omega_{en}|)\big](1-\Theta(\omega_{en})) \quad (9)$$

Whereas the distance dependent atomic level linewidth is given by:

$$\delta\Gamma(z) = 2\sum_n \mu_\alpha^{gn}\mu_\beta^{ng} Im\big[G_{\alpha\beta}(z;|\omega_{en}|)\big](1-\Theta(\omega_{en})) \quad (10)$$

Here the summation is considered to be over all allowed dipole couplings. The transition frequencies ω_{gn} or ω_{en} are considered positive for upward couplings and negative for downward couplings. $\Theta(\omega_{en})$ is the Heaviside function, ξ is an integration variable, μ_α^{gn}, μ_β^{ng}, μ_α^{en}, μ_β^{ne} are the dipole moment matrix elements and $G_{\alpha\beta}(z,i\xi)$ is the linear susceptibility function defined in [33], [34], [36]. We use the Einstein notation, implying a summation over the index variables α and β that denote the Cartesian coordinate components. In the near field the linear susceptibility is a diagonal matrix whose elements are proportional to $\frac{1}{(2z)^3}\frac{\varepsilon(\omega)-1}{\varepsilon(\omega)+1}$.

References and Notes

[1] H. B. G. Casimir and D. Polder, "The Influence of Retardation on the London-van der Waals Forces," *Phys. Rev.*, vol. 73, no. 4, pp. 360–372, Feb. 1948.

[2] M. Oria, M. Chevrollier, D. Bloch, M. Fichet, and M. Ducloy, "Spectral Observation of Surface-Induced Van der Waals Attraction on Atomic Vapour," *Europhys. Lett. EPL*, vol. 14, no. 6, pp. 527–532, Mar. 1991.

[3] M. Chevrollier, M. Fichet, M. Oria, G. Rahmat, D. Bloch, and M. Ducloy, "High resolution selective reflection spectroscopy as a probe of long-range surface interaction : measurement of the surface van der Waals attraction exerted on excited Cs atoms," *J. Phys. II*, vol. 2, no. 4, pp. 631–657, Apr. 1992.

[4] M. Fichet *et al.*, "Exploring the van der Waals atom-surface attraction in the nanometric range," *Europhys. Lett. EPL*, vol. 77, no. 5, p. 54001, Mar. 2007.

[5] V. Sandoghdar, C. I. Sukenik, E. A. Hinds, and S. Haroche, "Direct measurement of the van der Waals interaction between an atom and its images in a micron-sized cavity," *Phys. Rev. Lett.*, vol. 68, no. 23, pp. 3432–3435, Jun. 1992.

[6] C. I. Sukenik, M. G. Boshier, D. Cho, V. Sandoghdar, and E. A. Hinds, “Measurement of the Casimir-Polder force,” *Phys. Rev. Lett.*, vol. 70, no. 5, pp. 560–563, Feb. 1993.
[7] A. Landragin, J.-Y. Courtois, G. Labeyrie, N. Vansteenkiste, C. I. Westbrook, and A. Aspect, “Measurement of the van der Waals Force in an Atomic Mirror,” *Phys. Rev. Lett.*, vol. 77, no. 8, pp. 1464–1467, Aug. 1996.
[8] H. Bender, P. W. Courteille, C. Marzok, C. Zimmermann, and S. Slama, “Direct Measurement of Intermediate-Range Casimir-Polder Potentials,” *Phys. Rev. Lett.*, vol. 104, no. 8, Feb. 2010.
[9] J. M. Obrecht, R. J. Wild, M. Antezza, L. P. Pitaevskii, S. Stringari, and E. A. Cornell, “Measurement of the Temperature Dependence of the Casimir-Polder Force,” *Phys. Rev. Lett.*, vol. 98, no. 6, Feb. 2007.
[10] D. J. Alton *et al.*, “Strong interactions of single atoms and photons near a dielectric boundary,” *Nat. Phys.*, vol. 7, no. 2, pp. 159–165, Feb. 2011.
[11] M. Gullans *et al.*, “Nanoplasmonic Lattices for Ultracold Atoms,” *Phys. Rev. Lett.*, vol. 109, no. 23, Dec. 2012.
[12] A. Goban *et al.*, “Superradiance for Atoms Trapped along a Photonic Crystal Waveguide,” *Phys. Rev. Lett.*, vol. 115, no. 6, Aug. 2015.
[13] E. Vetsch, D. Reitz, G. Sagu?, R. Schmidt, S. T. Dawkins, and A. Rauschenbeutel, “Optical Interface Created by Laser-Cooled Atoms Trapped in the Evanescent Field Surrounding an Optical Nanofiber,” *Phys. Rev. Lett.*, vol. 104, no. 20, May 2010.
[14] S. Okaba *et al.*, “Lamb-Dicke spectroscopy of atoms in a hollow-core photonic crystal fibre,” *Nat. Commun.*, vol. 5, Jun. 2014.
[15] J. D. Thompson *et al.*, “Coupling a Single Trapped Atom to a Nanoscale Optical Cavity,” *Science*, vol. 340, no. 6137, pp. 1202–1205, Jun. 2013.
[16] D. E. Chang, K. Sinha, J. M. Taylor, and H. J. Kimble, “Trapping atoms using nanoscale quantum vacuum forces,” *Nat. Commun.*, vol. 5, Jul. 2014.
[17] A. Goban *et al.*, “Atom–light interactions in photonic crystals,” *Nat. Commun.*, vol. 5, May 2014.
[18] S.-P. Yu *et al.*, “Nanowire photonic crystal waveguides for single-atom trapping and strong light-matter interactions,” *Appl. Phys. Lett.*, vol. 104, no. 11, p. 111103, Mar. 2014.
[19] H. Failache, S. Saltiel, M. Fichet, D. Bloch, and M. Ducloy, “Resonant van der Waals Repulsion between Excited Cs Atoms and Sapphire Surface,” *Phys. Rev. Lett.*, vol. 83, no. 26, pp. 5467–5470, Dec. 1999.
[20] H. Failache, S. Saltiel, M. Fichet, D. Bloch, and M. Ducloy, “Resonant coupling in the van der Waals interaction between an excited alkali atom and a dielectric surface: an experimental study via stepwise selective reflection spectroscopy,” *Eur. Phys. J. - At. Mol. Opt. Phys.*, vol. 23, no. 2, pp. 237–255, May 2003.
[21] A. Laliotis, T. P. de Silans, I. Maurin, M. Ducloy, and D. Bloch, “Casimir–Polder interactions in the presence of thermally excited surface modes,” *Nat. Commun.*, vol. 5, Jul. 2014.
[22] M.-P. Gorza, S. Saltiel, H. Failache, and M. Ducloy, “Quantum theory of van der Waals interactions between excited atoms and birefringent dielectric surfaces,” *Eur. Phys. J. D*, vol. 15, no. 1, pp. 113–126, Jul. 2001.
[23] L. Stern, M. Grajower, and U. Levy, “Fano resonances and all-optical switching in a resonantly coupled plasmonic–atomic system,” *Nat. Commun.*, vol. 5, p. 4865, Sep. 2014.
[24] S. A. Aljunid, E. A. Chan, G. Adamo, M. Ducloy, D. Wilkowski, and N. I. Zheludev, “Atomic Response in the Near-Field of Nanostructured Plasmonic Metamaterial,” *Nano Lett.*, vol. 16, no. 5, pp. 3137–3141, May 2016.
[25] M. Ducloy and M. Fichet, “General theory of frequency modulated selective reflection. Influence of atom surface interactions,” *J. Phys. II*, vol. 1, no. 12, pp. 1429–1446, Dec. 1991.
[26] H. Failache, S. Saltiel, A. Fischer, D. Bloch, and M. Ducloy, “Resonant Quenching of Gas-Phase Cs Atoms Induced by Surface Polaritons,” *Phys. Rev. Lett.*, vol. 88, no. 24, May 2002.

[27] J. P. Woerdman and M. F. H. Schuurmans, “Spectral narrowing of selective reflection from sodium vapour,” *Opt. Commun.*, vol. 14, no. 2, pp. 248–251, Jun. 1975.
[28] A. M. Akulshin *et al.*, “Collisional Broadening of Intra-Doppler Resonances of Selective Reflection on the D2 Line of Cesium,” *Jetp Letters*, pp. 303–307, 1975.
[29] X. Chen, T. M. Grzegorczyk, B.-I. Wu, J. Pacheco, and J. A. Kong, “Robust method to retrieve the constitutive effective parameters of metamaterials,” *Phys. Rev. E*, vol. 70, no. 1, Jul. 2004.
[30] J. Baker-Jarvis, E. J. Vanzura, and W. A. Kissick, “Improved technique for determining complex permittivity with the transmission/reflection method,” *IEEE Trans. Microw. Theory Tech.*, vol. 38, no. 8, pp. 1096–1103, Aug. 1990.
[31] C. Stehle, C. Zimmermann, and S. Slama, “Cooperative coupling of ultracold atoms and surface plasmons,” *Nat. Phys.*, vol. 10, no. 12, pp. 937–942, Oct. 2014.
[32] G. M. Akselrod , C. Argyropoulos, T. B. Hoang, C. Ciracì, C. Fang, J. Huang, D. R. Smith and M. H. Mikkelsen, “Probing the mechanisms of large Purcell enhancement in plasmonic nanoantennas,” *Nat. Photonics*, vol. 8, no. 11, pp. 835–840, Oct. 2014.
[33] J. M. Wylie and J. E. Sipe, “Quantum electrodynamics near an interface,” *Phys. Rev. A*, vol. 30, no. 3, pp. 1185–1193, Sep. 1984.
[34] J. M. Wylie and J. E. Sipe, “Quantum electrodynamics near an interface. II,” *Phys. Rev. A*, vol. 32, no. 4, pp. 2030–2043, Oct. 1985.
[35] M. Fichet, F. Schuller, D. Bloch, and M. Ducloy, “van der Waals interactions between excited-state atoms and dispersive dielectric surfaces,” *Phys. Rev. A*, vol. 51, no. 2, pp. 1553–1564, Feb. 1995.
[36] A. Laliotis and M. Ducloy, “Casimir-Polder effect with thermally excited surfaces,” *Phys. Rev. A*, vol. 91, no. 5, May 2015.
[37] F. Intravaia *et al.*, “Strong Casimir force reduction through metallic surface nanostructuring,” *Nat. Commun.*, vol. 4, Sep. 2013.
[38] H. B. Chan *et al.*, “Measurement of the Casimir Force between a Gold Sphere and a Silicon Surface with Nanoscale Trench Arrays,” *Phys. Rev. Lett.*, vol. 101, no. 3, Jul. 2008.
[39] H. Bender *et al.*, “Probing Atom-Surface Interactions by Diffraction of Bose-Einstein Condensates,” *Phys. Rev. X*, vol. 4, no. 1, Feb. 2014.
[40] M. Chevrollier, M. Oriá, J. G. de Souza, D. Bloch, M. Fichet, and M. Ducloy, “Selective reflection spectroscopy of a resonant vapor at the interface with a metallic layer,” *Phys. Rev. E*, vol. 63, no. 4, Mar. 2001.

Acknowledgments

A.L. thanks the UMI Majulab and the Centre for Quantum Technologies for supporting his trip to Singapore. We wish to thank N. I. Zheludev and E. Lassalle for fruitful discussions. **Funding:** This work was supported by the Singapore Ministry of Education Academic Research Fund Tier (grant no. MOE2011-T3-1-005). **Author contributions**: E.A.C. and S.A.A. performed the SR spectroscopy measurements. G.A. designed and fabricated the metamaterial. E.A.C., S.A.A., A.L., M.D., and D.W. conducted the data analysis. A.L., M.D., and D.W. established the theoretical model and the physical interpretations. D.W. coordinated the project and is responsible for all the materials disclosed in the paper and/or the Supplementary Materials. All authors participated in the writing of the manuscript. **Competing interests:** The authors declare that they have no competing interests. **Data and materials availability:** All data needed to evaluate the conclusions in the paper are present in the paper and/or the Supplementary Materials. Additional data related to this paper may be requested from the authors.

Figures and Tables

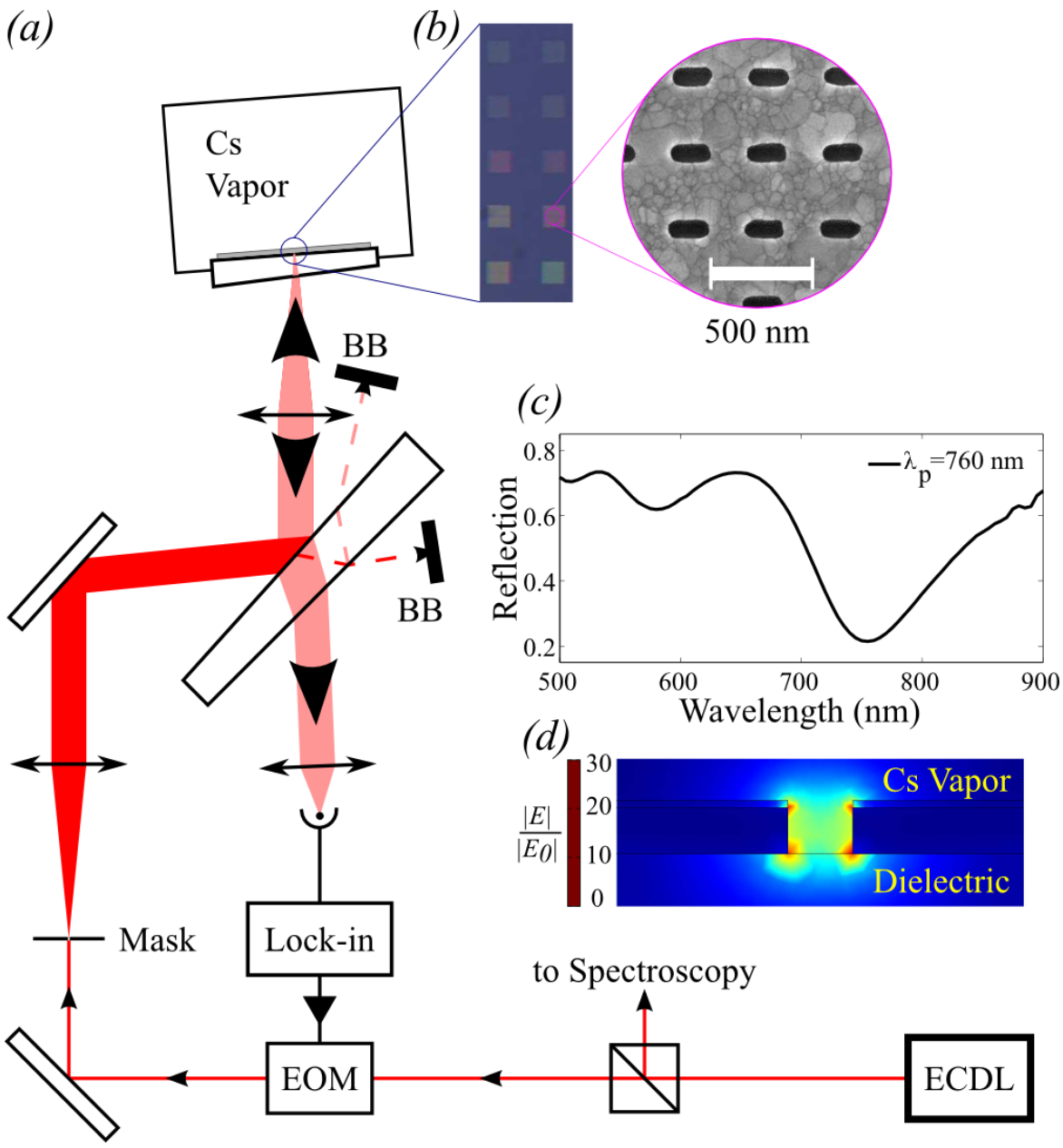

Fig. 1. Schematic of the experimental set-up. (a) Experimental set-up. (b) Real color back-illuminated images of the ten metamaterials. The zoom corresponds to an SEM image. (c) A typical reflectance curve of a metamaterial showing a main plasmon resonance at λ=760nm. (d) Cut along one nanoslit. The false colors represent the electric field magnitude, normalized by the amplitude of the incident field, as obtained by FDFD simulation. EOM, electro-optic modulator; BB, beam block

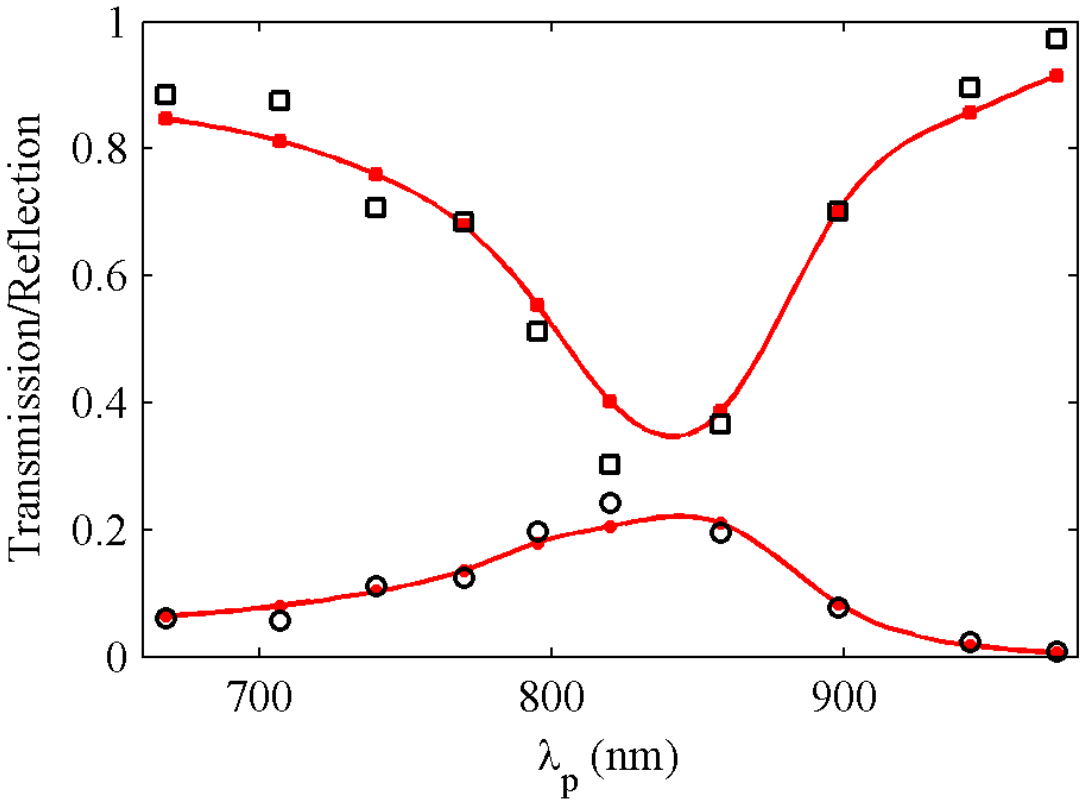

Fig. 2. Optical characterization of the metamaterials. Experimental reflection (open squares) and transmission (open circles) of the ten metamaterials measured with the 852nm laser. The x-axis corresponds to λ_p, the position of the plasmon resonance of each metamaterial. The solid red squares (circles) corresponds to the reflection (transmission) obtained by FDFD numerical simulation. The lines, connecting FDFD results, are guides for the eye.

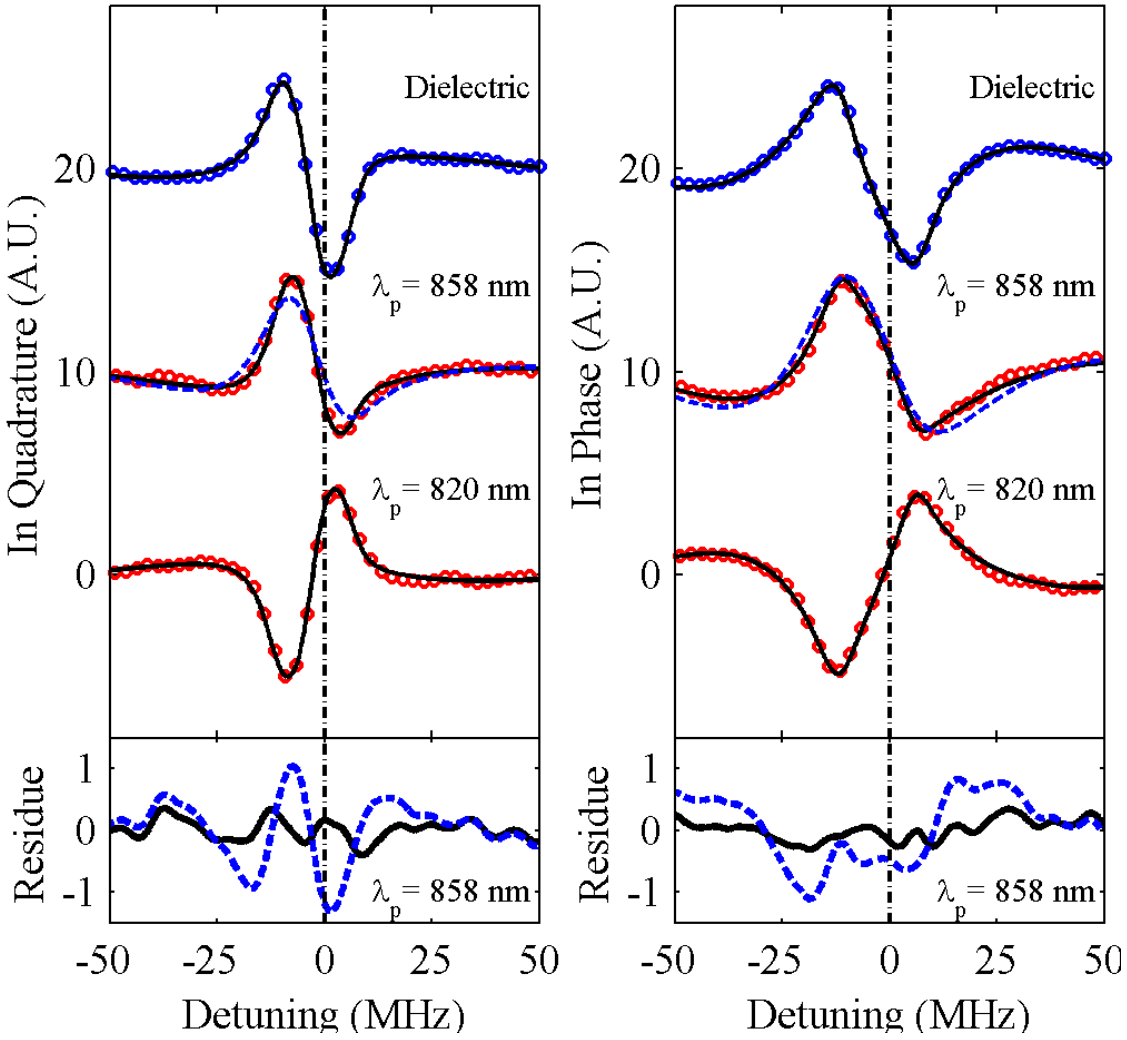

Fig. 3. Selective reflection spectra. In phase and in quadrature SR spectra of the plain windows (blue dots at top curves) and of two metamaterials (red dots). More spectra are shown in the Supplementary Materials. The black solid curves are the fits using Eqn.1. The dashed blue line is a fit assuming $\mathrm{Im}[\Delta C_3]=0$ for the metamaterial at λ_p=858nm. The residues correspond to the metamaterial at λ_p=858nm. The units are the same than for the main top curves. A.U., arbitrary units

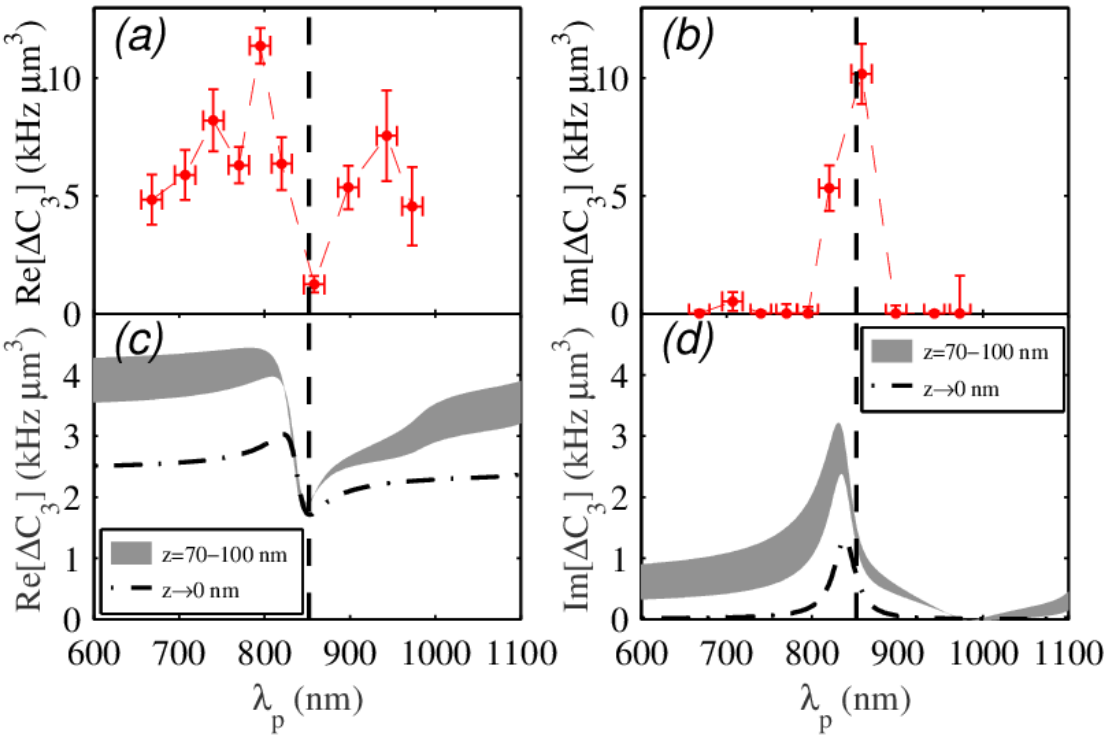

Fig. 4. The van der Waals coefficient. ΔC_3 coefficients as function of λ_p, the position of the plasmon resonance. Real part (a) and imaginary part (b) extracted from the fits of the SR signals. (c) and (d) are the real and imaginary parts of the C_3 coefficients computed from the model. The dot-dashed curve corresponds the non-retarded case ($z \rightarrow 0$). The retarded contribution is taken into account by considering an effective distance ranging from 70nm to 100nm. It correspond to the shaded grey surface. The vertical dashed lines indicate the position of the atomic resonance.